Shaking table testing on pile response due to lateral spreading

Jiunn-Shyang Chiou[1], T.-J. Huang[1], and C.-H. Chen[2]

[1] Department of Civil Engineering, National Taiwan University, 1, Sec. 4, Roosevelt Rd., Taipei 10617, Taiwan.
[2] National Center for Research on Earthquake Engineering, 200, Sec. 3, Xinhai Rd., Taipei, 10668, Taiwan.

ABSTRACT

Liquefaction-induced lateral spreading may cause significant damage to piles during an earthquake. In order to investigate the pile response subjected to lateral spreading, this study performed a shaking table test on two types of singe piles in a sloped ground with an inclination angle 2˚. An aluminum pile and a polypropylene pile were used to represent different pile stiffnesses. The piles were embedded in a multi-layered soil that was a dry sand layer underlain by a saturated layer and a clay layer was sandwiched between them. The test results showed the two piles had quit different displacement and moment responses under an input motion using the 1999 Taiwan ChiChi earthquake record at WuFeng.

Keywords: lateral spreading, piles; shaking table tests

1 INTRODUCTION

Past earthquake events have shown that pile foundations are often damaged due to liquefaction-induced lateral spreading (Yasuda and Berrill, 2000; GEER, 2010). In seismic design code of Taiwan, following the bridge design code of Japan (JRA, 2012), an equivalent lateral spread loading model is proposed for pile design. The formulas for the lateral spreading pressure in the model were developed based on only one case analysis for the 1995 Japan Hyogoken-Nanbu earthquake (Tokimatsu and Asaka, 1998). Therefore, the model needs more validation to have rational and safe design results in liquefaction resistant foundation design.

For piles in liquefiable soil, there are two major conditions for lateral spreading loading: (1) a uniform soil layer and (2) a non-uniform soil in which a liquefiable soil is overlain by a non-liquefiable soil. For the first condition, the lateral loading comes from the liquefied soil while for the second condition, without a thick liquefied soil layer, the lateral spreading loading can be as large as the passive soil pressure of the upper non-liquefied soil layer triggered by the movement of the underlain liquefied soil layer. Due to the large passive soil pressure, the second condition is a common cause of pile damage during an earthquake.

To investigate the behavior of single piles founded in liquefiable inclined soil, this study utilized the shaking table of the National Center for Research on Earthquake Engineering (NCREE) as well as a large scale laminar shear box developed by NCREE to perform a 1g dynamic model test. In this experimental study, a ground with an inclined angle of 2˚ was set. Focusing on the aforementioned second types of spreading load condition, a multi-layered sloped soil was designed: the bottommost layer of soil was a saturated loose sand for a liquefiable soil, the upmost layer was dry sand for a non-liquefiable crust, and a clay layer was sandwiched between them, acting as an impervious soil layer. Two single piles with different stiffnesses were used for comparing their performance: an aluminum pipe pile for a stiff pile and a polypropylene pile for a soft pile.

This paper presents the results of the test. A preliminary analysis is conducted to examine the applicability of the lateral spreading pressure formulas in the design code.

2 MODEL DESIGN AND PREPARATION

In this study, a sloped ground with an inclined angle of 2˚ was designed as shown in Fig. 1. A three-layer soil was considered: the lowest layer of soil was a saturated loose sand with a thickness of 100 cm, the topmost layer was dry sand with a thickness of 35 cm, and a thin clay layer of thickness 5 cm was placed between them to be an impervious layer for producing a water film beneath the clay layer to make the top dry sand layer slide along this interface during shaking. Vietnam sand was used for the sand layers and Kaolinite clay was used for the clay layer. Two single piles with different flexural stiffnesses were used: an aluminum pipe pile (AL pile) for a stiff pile and a polypropylene pile (PP pile) for a soft pile. The properties of the AL and PP piles are summarized in Table 1.

A laminar box was adopted to prepare the model. The two piles were fixed at the bottom of the box. The saturated sand layer then was prepared by the wet

pluviation method. The box was filled with water first and then the sand was pluviated into the water through an automated pluviation device. After that, the sand surface was slightly scraped to be a slope. Next, the dry clay and sand layers were prepared consecutively by manual pluviation using a funnel. The surfaces of the clay and dry sand layers were also scraped to be an inclined plane with the set inclined angle. The finished model for the test is displayed in Fig. 2.

Accelerometers were placed in the soil, on the piles, and on the frames of the laminar box to record the movement of the soil, piles, and frames. Piezometer arrays were placed in the soil to measure the pore water pressure, and the strain gauges and earth pressure cells were attached on the piles to measure the internal forces in and the earth pressures on the piles.

3 INPUT MOTIONS FOR SHAKING TABLE TESTING

The 1999 Taiwan ChiChi earthquake record at WuFeng (CWB24-WWF) was adopted for the main input motion for the shaking table test. The acceleration history of this record is as shown in Fig. 3. The maximum acceleration was -0.168 g and the duration was 70 sec. Before and after the main event, three events using white noise signals were applied to detect the dynamic characteristics of the system for different stages.

Table 1. Properties of AL and PP piles.

Item	AL pile	PP pile
Diameter (mm)	100	100
Wall thickness (mm)	3	-
Length (mm)	1600	1600
Unit weight (t/m^3)	2.711	0.89
Flexural rigidity (kNm^2)	75	9.72

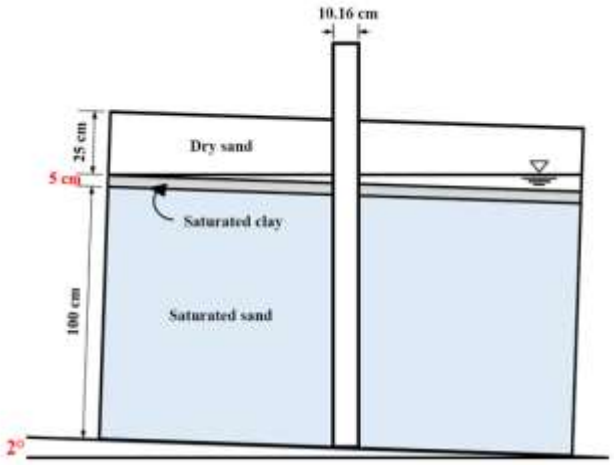

Fig. 1. Soil profile of inclined ground.

Fig. 2. Finished model of the shaking table test.

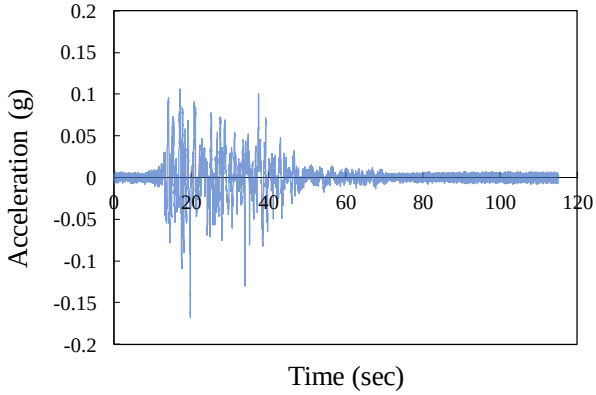

Fig. 3. Acceleration history of ChiChi earthquake (CWB24-WWF).

4 RESULTS

4.1 White noise signals

Three white noise events were applied for identifying the system characteristics under the following conditions: (1) piles without surrounding soil, (2) before the main event, and (3) after the main event. At the first condition, the system frequencies of the PP and AL piles were 8.69 and 23.4 Hz, respectively. At the second condition, the system frequencies of the PP and AL piles and soil layer were 14.8, 14.4, and 14.33 Hz. At the third condition, the system frequencies of the PP and AL piles and soil layer were 14.8, 14.1, and 14.76 Hz, respectively.

4.2 Historic earthquake

In the beginning of shaking, the soil did not have large displacements because of smaller accelerations, and the PP and AL piles did as well. With the increasing shaking intensity, the PP and AL piles began to displace more and the displacement of the PP pile was larger than the AL pile. During this period, the impervious effect of the clay was greatly influenced due to the back and forth movement of the piles.

Because of this, the relative displacement between the piles and the box bottom increased and soil was significantly squeezed so that at time about 28 sec, some sand or clay erupted and at time about 39 sec, a large amount of clay eruption occurred in front of the PP pile. The eruption of sand or clay continued even the shaking stopped. At time 76 sec, the piping stopped and the water flew back to the hole at the downslope side of the pile. After the shaking, the soil around the piles settled as shown in Fig. 4, in which the range of settlement of the PP pile was larger than that of the AL pile. It also can be seen that some clay flocs were on the soil surface.

Fig. 5 displays the histories of relative displacement between the pile top and bottom for the PP and AL piles. The maximum relative displacement of the AL pile was 29.68 mm at time 19.355 sec; the maximum relative displacement of the AL pile was 46.33 mm at time 19.39 sec. The difference of the relative displacement of the two piles was 16.65 mm.

Fig. 4. Soil surface condition after shaking.

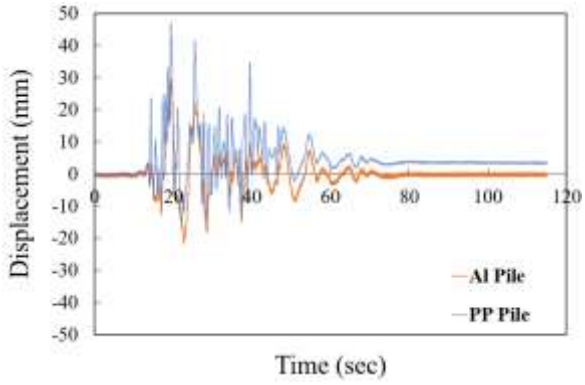

Fig. 5. Relative displacement histories of AL and PP piles.

Fig. 6 displays the histories of excess pore water pressure ratio (excess pore pressure divided by effective overburden pressure) at depths of 27, 57 and 87 mm. The ratios of the three depths were close to one at time 13.92 sec, keeping constant, implying the soil at these depths liquefied at this moment. Then, at the elevation 22 mm, the ratio decreased at time 28 sec. This may be due to that the drainage of water through the breakage of the clay layer since at this time the flowing phenomenon was observed.

The maximum moment occurred at 27.705 sec and 21.145 sec for the AL and PP piles, respectively. Fig. 7 displays the moment profiles with depth at the maximum moment. It is observed that below the elevation 100 mm (the interface of the clay and saturated sand), the moments were significant and the base of the piles sustained the maximum moment. The base moments of the PP pile and AL pile were about 0.482 and 0.989 kN-m, respectively.

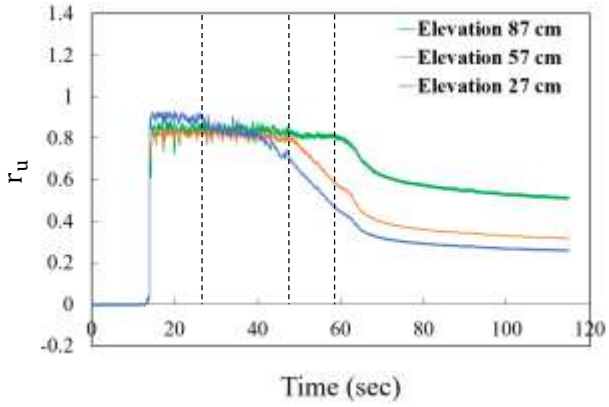

Fig. 6. Excess pore pressure ratio at different elevations.

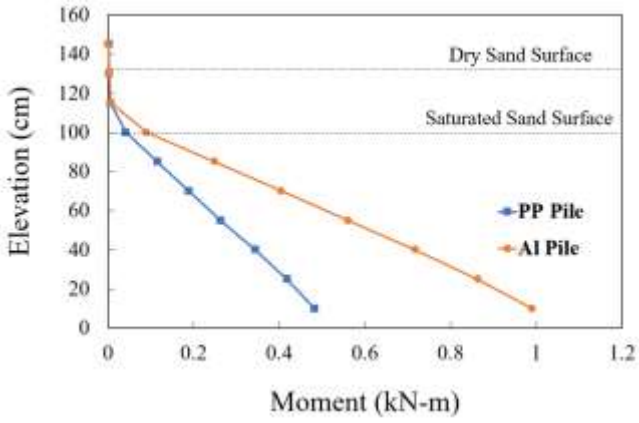

Fig. 7. Moment profile with depth at the time of maximum base moment.

For a liquefied soil overlain a non-liquefied soil, the spreading pressure on the pile can be computed based on the following equations as suggested in the specifications of Japan Road Association (JRA, 2012):

$$q_{NL} = C_s C_{NL} K_p \gamma_{NL} \ (0 \le x \le H_{NL}) \quad (1)$$

$$q_L = C_s C_L \{\gamma_{NL} H_{NL} + \gamma_L (x - H_{NL})\} \ (H_{NL} < x \le H_{NL} + H_L) \quad (2)$$

where q_{NL} and q_L are the lateral spreading pressures on the pile for the non-liquefied and liquefied layers, respectively; x is the depth; H_{NL} and H_L are the thicknesses of the non-liquefied and liquefied layers, respectively; γ_{NL} and γ_L are the unit weights of the non-liquefied and liquefied layers; K_p is the passive earth pressure coefficient; C_s is the modification factor on the distance to the waterfront; C_{NL} and C_L are the modification factors for the lateral spreading pressures of the non-liquefied and liquefied layers, respectively.

Using the above equations to estimate the pile responses and setting C_s, C_{NL}, and C_L to be one gives the lateral pressure on the pile as shown in Fig. 8. Accordingly, applying this spreading pressure on the PP and AL piles yields the moment distribution profiles for the PP and AL piles as shown in Figs. 9. Compared to the measured moment, for the PP pile, above the elevation 30 cm, the analysis moments are lower than the measured, but below the elevation 30 cm, the analysis moments are much larger than the measured; for the AL pile, the analysis moments are much smaller than the measured.

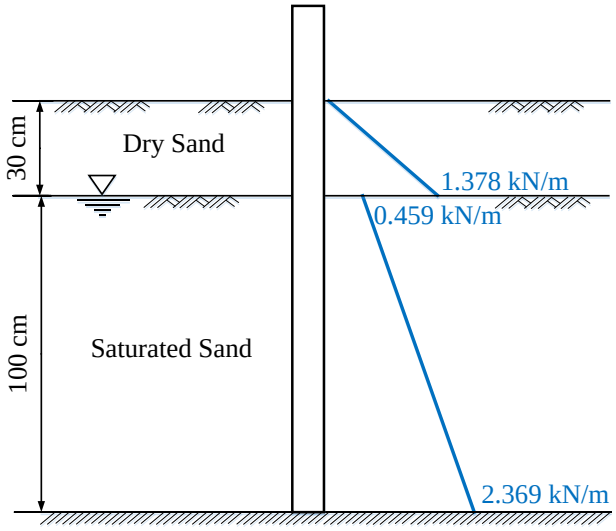

Fig. 8. Analysis lateral spreading pressures on the pile.

CONCLUSION

The following conclusions can be drawn:

(1) The moment responses for the piles of different stiffnesses are different. Generally, the stiff pile (AL pile) has a larger moment, implying a larger lateral spreading pressures on the pile.

(2) The JRA formulas for the lateral spreading pressure cannot discern the difference of the pile stiffness. In this case, for the PP pile, the JRA moments are lower than the measured for the shallow soil, but larger than the measured for the deep soil; for the AL pile, the JRA moments are much smaller than the measured for all depths of soil.

(3) The moment distribution below the interface of the soil and clay are approximately linear, implying the strength of soil is almost zero for the liquefied soil.

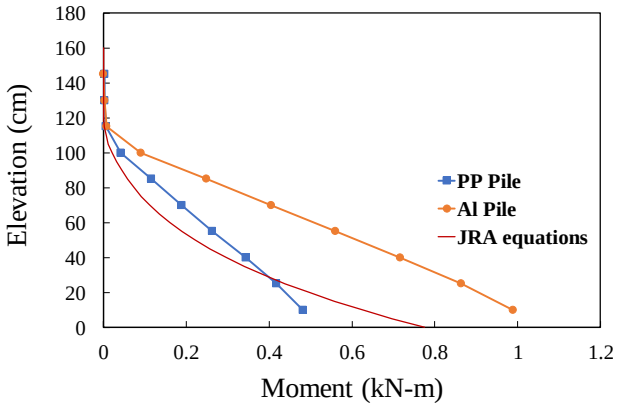

Fig. 9. Comparisons of analysis moment profile with the measured moment profiles for PP and AL piles.

ACKNOWLEDGEMENTS

The authors would like to thank the Ministry of Science and Technology of Taiwan (Grant no. MOST MOST 105-2625-M-002-024) and National Taiwan University (Grant no. NTUCC-107L892507) for financial support.

REFERENCES

Japan Road Association (JRA) (2012). Design Specifications for Highway Bridges - IV: Substructures. (in Japanese).

Yasuda S., and Berrill J. (2000). Observations of the earthquake response of foundations in soil profiles containing saturated sands. In: 1st International Conference on Geotechnical and Geological engineering, Melbourne, Australia, 1441–1471.

GEER. (2010). Geotechnical reconnaissance of the 2010 Darfield (New Zealand) earthquake. Technical Report. Association Report No. GEER-024, Version1: November 14, 2010; Geo-Engineering Extreme Events Reconnaissance.

Tokimatsu K., and Asaka Y. (1998). Effects of liquefaction-induced ground displacements on pile performance in the 1995 Hyogoken–Nanbu earthquake. Soils and Foundations, Special Issue, 163-77.